YITP-20-117, IPMU 20-0098

Addressing H_0 tension by means of VCDM

Antonio De Felice,[1,*] Shinji Mukohyama,[1,2,†] and Masroor C. Pookkillath[1,‡]

[1] *Center for Gravitational Physics, Yukawa Institute for Theoretical Physics, Kyoto University, 606-8502, Kyoto, Japan*
[2] *Kavli Institute for the Physics and Mathematics of the Universe (WPI), The University of Tokyo, Kashiwa, Chiba 277-8583, Japan*

In this letter we propose a reduction of the H_0 tension puzzle by means of a theory of minimally modified gravity which is dubbed VCDM. After confronting the theory with the experiments, we find that the data allow for a low-redshift transition in the expansion history of the universe at either $z \simeq 0.3$ or $z \simeq 1.8$, corresponding to one of the two local minima of the total χ^2. From the bestfit values the total fitness parameter is improved by $\Delta\chi^2 \simeq 12$, for the data set considered. We then infer the local Hubble expansion rate today within this theory by means of low redshift Pantheon data. The resulting local Hubble expansion rate today is $H_0^{\rm loc} = 73.6 \pm 1.4$. We find the tension is reduced within the VCDM theory.

arXiv:2009.08718v5 [astro-ph.CO] 2 May 2021

The value of today's rate of expansion of the universe, H_0, has been measured, as a direct measurement, from low-redshift observations, namely, SH0ES [1], H0LiCOW [2], Megamaser Cosmology Project [3] (MCP) and Carnegie-Chicago Hubble Program (CCHP) Collaboration [4]. Among these observations SH0ES in particular has achieved a remarkable precision providing $H_0 = 74.03 \pm 1.42$ (in units of $\mathrm{km\,s^{-1}\,Mpc^{-1}}$). On the other hand, on assuming some theoretical model, H_0 can also be deduced from the measurement of temperature power spectra in the Cosmic Microwave Background (CMB) which is produced at the recombination time. The recent Planck Legacy 2018 release gives $H_0 = 67.04 \pm 0.5$, assuming the standard flat-ΛCDM model (non-flat versions are known to be strongly disfavored by other data, e.g. Baryon Acoustic Oscillations (BAO)) [5]. Hence, the tension between this theoretical model and experimental results adds up to more than 4σ's [6, 7].

However, the flat-ΛCDM could be representing only a first approximation to another, improved model of our universe. The VCDM theory, described in the following, was originally introduced for the purpose of seeking minimal theoretical deviations from the standard model of gravity and cosmology, i.e. General Relativity (GR) and ΛCDM, as it does not introduce any new propagating physical degrees of freedom in the gravity sector, but on the other hand, one can have, as we will show in the following, a non-trivial and interesting phenomenology.

In the VCDM theory [8], the cosmological constant Λ in the standard ΛCDM is promoted to a function $V(\phi)$ of a non-dynamical, auxiliary field ϕ. This theory of modified gravity breaks four dimensional diffeomorphism invariance at cosmological scales but keeps the three dimensional spatial diffeomorphism invariance. On doing so, the theory modifies gravity at cosmological scales while it only possess two gravitational degrees of freedom as in GR. In general this allows a spectrum of possibilities typically much larger than the case of a scalar-tensor theory. For the latter, the extra scalar degree of freedom leads to strong constraints not only on solar system scales (for which one needs the scalar to be very massive or to be shielded by some non-trivial dynamical mechanisms, e.g. chameleon or Vainshtein), but also on cosmological scales (for which one needs to constrain the background dynamics as to avoid ghost and gradient instabilities).

The equations of motion for the VCDM theory on a homogeneous and isotropic background can be written as

$$V = \frac{1}{3}\phi^2 - \frac{\rho}{M_{\rm P}^2}\,, \quad \frac{d\phi}{d\mathcal{N}} = \frac{3}{2}\frac{\rho+P}{M_{\rm P}^2 H}\,, \quad \frac{d\rho_I}{d\mathcal{N}} + 3(\rho_I + P_I) = 0\,, \tag{1}$$

where $\mathcal{N} = \ln(a/a_0)$ (a being the scale factor and a_0 being its present value), $H = \dot{a}/a^2$ is the Hubble expansion rate (a dot denotes differentiation with respect to the conformal time), $\rho = \sum_I \rho_I$ and $P = \sum_I P_I$ (the sum is over the standard matter species). Unless $\rho + P = 0$, the following equation follows from the above equations: $\phi = \frac{3}{2}V_{,\phi} - 3H$. When V is a linear function of ϕ, as in $V = \lambda_1\phi + \lambda_0$, then the equations of motion (1) reduce to

$$3H^2 = \frac{\rho}{M_{\rm P}^2} + \Lambda\,, \quad H\frac{dH}{d\mathcal{N}} = -\frac{\rho+P}{2M_{\rm P}^2}\,, \quad \frac{d\rho_i}{d\mathcal{N}} + 3(\rho_I + P_I) = 0\,, \tag{2}$$

where $\Lambda \equiv \lambda_0 + 3\lambda_1^2/4 = \text{const}$. These are nothing but the equations of motion in the standard ΛCDM model. Moreover, for this choice of $V(\phi)$ the theory reduces to GR with a cosmological constant not only for the homogeneous and isotropic background but also for perturbations at any order. Hence, the VCDM theory extends the ΛCDM model by replacing the constant Λ with a free function $V(\phi)$. Yet, the VCDM theory does not introduce extra degrees of freedom in the sense that the number of independent initial conditions is the same as ΛCDM. The "V" of VCDM therefore stands for the free function $V(\phi)$ introduced in this theory.

In the following we want to be able to use the free function $V(\phi)$ in order to give any wanted background evolution for H which can be given as $H = H(\mathcal{N})$. From the 2nd of (1), having given H as a function of $\mathcal{N}$, then

one obtains

$$\phi(\mathcal{N}) = \phi_0 + \int_{\mathcal{N}_0}^{\mathcal{N}} \frac{3}{2}\frac{\rho(\mathcal{N}') + P(\mathcal{N}')}{M_{\rm Pl}^2 H(\mathcal{N}')} d\mathcal{N}' \,, \qquad (3)$$

where $\phi_0 = \phi(\mathcal{N}_0)$. Assuming that $\rho + P > 0$, and $H > 0$, the right hand side of (3) is an increasing function of $\mathcal{N}$ and thus the function $\phi(\mathcal{N})$ has a unique inverse function, $\mathcal{N} = \mathcal{N}(\phi)$. Obviously, $\mathcal{N}$ is an increasing function of ϕ. By combining this with the 1st of (1), one obtains

$$V(\phi) = \frac{1}{3}\phi^2 - \frac{\rho(\mathcal{N}(\phi))}{M_{\rm Pl}^2} \,. \qquad (4)$$

Therefore we have obtained a simple and powerful reconstruction mechanism for V for a given and wanted evolution of H [1]. Once $V(\phi)$ is specified in this way, we know how to evolve not only the homogeneous and isotropic background but also perturbations around it.

Having shown the reconstruction of the potential V for a given evolution of H, we can search for a profile for $H(z)$ that can potentially reduce the H_0 tension. We introduce two choices of $H(z)$ to address current cosmological tensions: one in the flat-ΛCDM and the other in the VCDM. The former is $H_\Lambda^2 \equiv H_{\Lambda 0}^2[\tilde{\Omega}_\Lambda + \tilde{\Omega}_{m0}(1+z)^3 + \tilde{\Omega}_{r0}(1+z)^4]$, where $\tilde{\Omega}_\Lambda \equiv 1 - \tilde{\Omega}_{m0} - \tilde{\Omega}_{r0}$, and the latter is

$$H^2 = H_\Lambda^2 + A_1 H_0^2 \left[1 - \tanh\left(\frac{z - A_2}{A_3}\right)\right], \qquad (5)$$

with the idea that $0 < A_2 < 2$. In this case we have at early times, for $z \gg |A_2|$, that the system will tend to be the standard flat-ΛCDM evolution, i.e. $H^2 \approx H_\Lambda^2$. Today, i.e. for $z = 0$, we have $H_0^2 = H_\Lambda^2 + A_1 H_0^2 \left[1 + \tanh\left(\frac{A_2}{A_3}\right)\right]$, which can be solved today for A_1, to give $A_1 = (1 - H_{\Lambda 0}^2/H_0^2)\left[\tanh(A_2/A_3) + 1\right]^{-1}$.

Let us further consider the following parameter redefinitions $\tilde{\Omega}_{m0} = \Omega_{m0}\, H_0^2/H_{\Lambda 0}^2$, $\tilde{\Omega}_{r0} = \Omega_{r0}\, H_0^2/H_{\Lambda 0}^2$, and $\beta_H = H_{\Lambda 0}/H_0$, then we find[2]

$$\frac{H^2}{H_0^2} = \Omega_{\rm m0}(1+z)^3 + \Omega_{\rm r0}(1+z)^4 + (1-\beta_H^2)\frac{1 + \tanh\left(\frac{A_2 - z}{A_3}\right)}{1 + \tanh\left(\frac{A_2}{A_3}\right)} + \beta_H^2\left(1 - \frac{\Omega_{\rm m0}}{\beta_H^2} - \frac{\Omega_{\rm r0}}{\beta_H^2}\right) . \qquad (6)$$

So in total we have six background parameters (three more than ΛCDM). However, we can reduce them to five (two more than ΛCDM) by fixing A_3 as we expect to have a large degeneracy (after assuming $A_2 = \mathcal{O}(1)$). According to Akaike Information Criterion (AIC), we can accept the model if we can have an improvement of χ^2 larger than four in comparison with ΛCDM [9]. In fact, we will show later on that the χ^2 has improved by $\Delta\chi^2 \simeq 12$ with respect to ΛCDM. In particular, we will fix, later on, A_3 to the value of 10^{-3}.

Two things need to be noticed. First, having given the expression for $H = H(z)$, one can automatically deduce all the needed background expressions as well as all evolution equations for perturbations. Second, the fact we have a minimally modified gravity (VCDM)-component does not mean we are adding a physical dark-component degree of freedom. In fact, for this theory, there is no additional physical degree of freedom, beside the tensorial gravitational waves and the standard ones related to the presence of matter fields [8].

After having introduced the behavior of the VCDM model on a homogeneous and isotropic background, we will test it against several cosmological data to see how well it can address the H_0 tension. Here we use Planck Legacy 2018 data with `planck_highl_TTTEEE`, `planck_lowl_EE`, and `planck_lowl_TT` [10], baryon acoustic oscillation (BAO) from 6dF Galaxy Survey [11] and the Sloan Digital Sky Survey [12, 13], and Pantheon data set comprised of 1048 type Ia supernovae [14]. We use single data points of H_0 from SH0ES $H_0 = 73.2 \pm 1.3$ [15] (in standard units), H0LiCOW $H_0 = 73.3 \pm 1.8$ [2] and MCP $H_0 = 73.9 \pm 3$ [3]. We also add to the Pantheon likelihood a gaussian likelihood for the absolute magnitude M of the supernovae samples to properly account astrophysical independent input inside the context of the Hubble tension [16–19]. We then infer the local value of Hubble expansion today $H_0^{\rm loc}$ using the Pantheon data and employing the analysis technique explained in [16, 17]. Here we have not included the

[1] The potential $V(\phi)$ is not unique. Even for the same choice of $H(z)$, the shape of the potential $V(\phi)$ depends on the initial value of ϕ, which can be chosen arbitrarily. Changing the initial value of ϕ changes the potential V by a constant and a term linear in ϕ. In any case, the potential does not enter both at the level of the background and linear perturbation theory which are affected only by $H(z)$ and its derivatives. Furthermore, VCDM theory reduces to GR whenever $V_{,\phi\phi} = 0$. See e.g. eq. (5.11) of [8], which shows $w_\phi = -1$ whenever $V_{,\phi\phi} = 0$

[2] As for Montecarlo sampling, to make sure about convergence, we have also run the chains by redefining the parameter β_H as $\beta_H = (2 - \tilde{\beta}_H^2)^{-1/2}$ and have given a flat prior for the new parameter $\tilde{\beta}_H$.

Planck lensing data since it was reported that the lensing anomaly is present in the Plank legacy release [20, 21].

Both the background and linear perturbation equations of motion are implemented in the Boltzmann code CLASS [22], with covariantly corrected baryon equations of motion [23].

For a matter action at second order up to shear for a fluid we proceed here by first writing the Schutz-Sorkin Lagrangian (SSL) for a single fluid [23], as follows

$$S_{\rm SSL} = -\int d^4x\sqrt{-g}[\rho(n,s) + J^\mu\left(\partial_\mu\ell + \theta\partial_\mu s + A_1\partial_\mu B_1 + A_2\partial_\mu B_2\right)]\,, \tag{7}$$

with $n = \sqrt{-J^\mu J^\mu g_{\mu\nu}}$, and 4-velocity $u^\alpha = J^\alpha/n$. We consider several copies of the previous action each describing a different fluid, labeled with an index I. Then we can expand the previous SSL up to second order in the perturbation fields, and to this one, we then add a correction aimed to describe an anisotropic fluid as follows $S^{(2)}_{\rm m} = S^{(2)}_{\rm SSL} + S^{(2)}{}_{\rm corr}$, where $S^{(2)}{}_{\rm corr} = \int dtd^3xNa^3\sum_I \sigma_I\,\Theta_I$ and Θ_I stands for a linear combination of perturbation fields. Since for each matter species $\rho_I = \rho_I(n_I)$, and $n_I = \sqrt{-J^\mu_I J^\nu_I g_{\mu\nu}}$, one can find a relation among $\delta\rho_I$ and the other fields as $\delta J_I = \frac{\rho_I}{n_I\rho_{I,n}}\frac{\delta\rho_I}{\rho_I} - \alpha$, where $\delta N = N(t)\alpha$, which can be used as a field redefinition to replace δJ_I in terms of $\frac{\delta\rho_I}{\rho_I}$. We also define gauge invariant combinations $v_I = -\frac{a}{k^2}\theta_I + \chi - \frac{a^2}{N}\partial_t(E/a^2)$, $\alpha = \Psi - \frac{\dot\chi}{N} + N^{-1}\partial_t[a^2N^{-1}\partial_t(E/a^2)]$, and $\zeta = -\Phi - H\,\chi + \frac{a^2H}{N}\,\partial_t(E/a^2)$, where $\delta\gamma_{ij} = 2[a^2\zeta\delta_{ij} + \partial_i\partial_j E]$, and $\delta u_{Ii} = \partial_i v_I$. We find finally that

$$S^{(2)}_{\rm corr} = \int dtd^3x\,Na^3\sum_I \sigma_I\left[\delta\rho_I + 3\left(\rho_I + P_I\right)\zeta\right]. \tag{8}$$

For vector transverse modes, we can define $T^i_{Ij} \equiv P_I\,\delta^i{}_j + P_I\,\frac{\delta^{ik}}{a^2}\,\pi^I_{kj}$, and $\pi^I_{ij} \equiv \frac{1}{2}\left(\partial_i\pi^{I,T}_j + \partial_j\pi^{I,T}_i\right)$. Then we can introduce the 1+3 decompositions for the 4-velocity of the fluid $u^{V,I}_{Ii} = \delta u^I_{Ii}$, the shift $N_i = a\,N\,G_i$, and the 3D metric $\delta\gamma_{ij} = a\left(\partial_i C_j + \partial_j C_i\right)$. We can also introduce the following gauge invariant variables $V_i = G_i - \frac{a}{N}\frac{d}{dt}\left(\frac{C_i}{a}\right)$, and $F^I_i = \frac{C_i}{a} - \frac{b^I_{1i}}{\vec b^I_1\cdot\vec b^I_1}\,\delta B^I_1 - \frac{b^I_{2i}}{\vec b^I_2\cdot\vec b^I_2}\,\delta B^I_2$, where $b^I_{1i}b^I_{2i} = 0 = b^I_{1i}k^i = b^I_{2i}k^i$. Then, on following a similar approach one finds the total Lagrangian density for the vector perturbations, in VCDM, can be written as

$$\mathcal{L} = Na^3\delta^{ij}\left\{\sum_I n_I\rho_{I,n}\,\frac{\dot F^I_i}{N}\,\delta u^I_j + \frac{1}{a^2}\sum_I n_I\rho_{I,n}\left[a\delta u^I_i V_j - \frac{1}{2}\,\delta u^I_i\delta u^I_j\right] - \frac{M^2_{\rm P}}{4a^2}\,V_i(\delta^{lm}\partial_l\partial_m V_j)\right.$$
$$\left. - \frac{1}{2a^2}\sum_I P_I\,\pi^{I,T}_i\,(\delta^{lm}\partial_l\partial_m F^I_j)\right\}, \tag{9}$$

which reduces to the same result as in GR.

Finally, for the tensor modes, let us define $\delta\gamma_{ij} = a^2\left(h_+\varepsilon^+_{ij} + h_\times\varepsilon^\times_{ij}\right)$, where $\varepsilon^{+,\times}_{ij} = \varepsilon^{+,\times}_{ji}$, $\delta^{ij}\varepsilon^{+,\times}_{ij} = 0$, $\varepsilon^+_{ij}\varepsilon^\times_{mn}\delta^{im}\delta^{jn} = 0$, and $\varepsilon^+_{ij}\varepsilon^+_{mn}\delta^{im}\delta^{jn} = 1 = \varepsilon^\times_{ij}\varepsilon^\times_{mn}\delta^{im}\delta^{jn}$. As for the energy-momentum tensor we have instead for the perturbations $\delta T^i_{Ij} \equiv P_I\,\frac{\delta^{ik}}{a^2}\,\pi^{I,TT}_{kj}$, so that the total Lagrangian density in VCDM becomes

$$\mathcal{L} = \frac{M^2_{\rm P}}{8}\,\frac{a^3}{N}\,(\dot h^2_+ + \dot h^2_\times) - \frac{Na\,M^2_{\rm P}}{8}\left[(\partial_i h_+)\delta^{ij}(\partial_j h_+) + (\partial_i h_\times)\delta^{ij}(\partial_j h_\times)\right] + \frac{Na}{2}\sum_I P_I\left(h_+\pi^I_+ + h_\times\pi^I_\times\right), \tag{10}$$

which reduces to the same form of GR.

Before substituting the explicit dependence of H on the redshift z, all the equations of motion (including the ones for the matter fields) for the perturbations are, in form, exactly the same as for ΛCDM, except the following one (written in terms of the Newtonian-gauge invariant

fields Φ and Ψ):

$$\dot{\Phi}+aH\Psi = \frac{3\,[k^2-3a^2(\dot{H}/a)]}{k^2\,[2k^2/a^2+9\sum_K(\varrho_K+p_K)]}\,\sum_I(\varrho_I+p_I)\,\theta_I\,, \tag{11}$$

which is used to find the evolution of the curvature perturbation Φ, and where a dot represents a derivative with respect the conformal time. Here we have used CLASS notation, namely $\varrho_I = \rho_I/(3M_{\rm P}^2)$, $p_I = P_I/(3M_{\rm P}^2)$. At the level of linear perturbation, the deviation from ΛCDM therefore consists of two parts: the explicit difference seen in (11) and the implicit difference due to different $H(z)$.

The parameter estimation is made via Markov Chain Monte Carlo (MCMC) sampling by using Monte Python [24, 25] against the above mentioned data sets. In the MCMC sampling we used very high precision by decreasing the step size for both background and perturbation integration[3] to see the smooth transition of $H(z)$ for both VCDM and ΛCDM. The analysis of the MCMC chains is performed using a chain analyzer package, GetDist [26].

We have considered the prior for the parameters of VCDM such that ΛCDM is well inside the region. (We will see later on that there are two local minima of the total χ^2, corresponding to transitions at redshift $z \simeq 0.3$ (low-z) and $z \simeq 1.8$ (high-z), respectively). In particular, for low-z we give the following priors: $0.6 < \beta_H < 1.3$, and $0.15 < A_2 < 0.4$. For high-z we give $0.05 < \beta_H < 2.3$ ($\beta_H \to 0$ just implies that the amount of amplitude transition is finite), and $0.4 < A_2 < 5$. We fix $A_3 = 10^{-3}$ as it has large degeneracy in both low-z and high-z. Deviations of β_H from 1 imply that the cosmological data sets prefer the VCDM model over ΛCDM.

By doing the chain analysis we found that, on using only Planck-BAO-Pantheon data alone, VCDM shows two minima: one has a value of $\beta_H \simeq 0.94$, and the other one has a lower value of β_H. The two minima (for the χ^2-function) differ, among other things, on the value for the redshift at which the VCDM model shows the transition for $H(z)$.

In order to discriminate between these two minima, we also add to the previous data sets three robust measurements of H_0, namely SH0ES, H0LiCOW and MEGAMASER. On doing this, both minima still remain, but, in any case, the total χ^2 clearly favors VCDM, as $\beta_H < 1$ at 2σ, whereas ΛCDM still gives a much lower value for h_0 giving rise to the well-known tension among data sets.

One may wonder whether the data still point towards other possible features which the chosen $H(z)$ (for this project) for VCDM might not be able to fully implement. If in the near future more and more data will be pointing towards some non-trivial features for $H(z)$, VCDM (with practically for any chosen, but positive, $H(z)$), has to be considered as a solid playground with which one can test modified background cosmological evolutions. In order to have a better picture of the χ^2 for the cosmological data sets we have considered, in Table I, we compare the contribution to the χ^2 from each experiment between VCDM and ΛCDM and also show the residue $\Delta\chi^2$. Furthermore, since we find that at 2σ $A_2 > 0.24$ (A_2 fixes the redshift of the transition for $H(z)$ to a larger value of H), the VCDM theory combined with the cosmological data sets automatically avoids the potential problem of a transition around $z = 0$ as explained in [17].

Fig. 1 shows 2-dimensional marginalised likelihoods for the cosmological parameters of interest in VCDM model as well as for ΛCDM. The Table II gives the values of the parameters within 2σ's. It is clear that the parameter A_2 has a sharp upper cut off. This can be understood by the following logic. Both BAO and Planck data have a better fit for a dynamics for $H(z)$ which leads to lower values of H_0 (compared to local measurements in ΛCDM). This behavior still holds for VCDM. But for lower redshifts (outside the range of BAO-dr12, for which $0.38 < z < 0.61$), Pantheon data require larger values for $H(z)$, and the transition occurs. In order to take into account lower redshift BAO data, we have also considered small-z BAO data (refer to table I). This explains the redshift of transition (related to the A_2 parameter), and probably some similar behavior will be required if both current and future cosmological data will keep constraining the ΛCDM profile for $H(z)$. As for the width of the transition (related to the A_3 parameter, we have fixed it to the value of 10^{-3}. This does not lead to a fine-tuning: it is just a choice. In fact, if we perform a Montecarlo sampling by adding this third parameter, we find for the same wanted value of H_0 a large degeneracy (about three orders of magnitude at 1σ) for A_3 (see Fig. 2). This only shows that the data are still not powerful enough to give some insight into this parameter. For this reason, we have fixed A_3 to a reasonable value.

From Table II, it is interesting to notice that the value of β_H does not reach 1 even at 2σ. It means that the data prefer VCDM over ΛCDM. We find that the bestfit value of Hubble expansion rate today is $H_0 = 70.83$ and $H_0 = 70,49$ for low$-z$ and high$-z$ respectively, which indicates that the tension is reduced. However we need to determine the local value of the Hubble expansion rate today $H_0^{\rm loc}$ following the analysis explained in [16, 17] (refer to Appendix A for details). We find that the local value of the Hubble expansion today is $H_0^{\rm loc} = 73.6 \pm 1.4$. Fig. 3 shows the contour of Ω_m and H_0 determined by the MCMC analysis and also the $H_0^{\rm loc}$ with 2σ error bars.

Let us look at the behavior of $H(z)$ in VCDM. Fig.4, shows the two independent transitions at $z \simeq 3$ and

[3] More in detail we have set in CLASS the variables `tol_perturb_integration, tol_background_integration` to 10^{-12}, `back_integration_stepsize, perturb_integration_stepsize` to 10^{-4}, etc.

Experiments	**ΛCDM**	**VCDM low$-z$ ($\Delta\chi^2$)**	**VCDM high$-z$ ($\Delta\chi^2$)**
Planck_highl_TTTEEE	2354.01	2349.56 (4.45)	2347.03 (6.98)
Planck_lowl_EE	397.37	395.92 (1.45)	395.83 (1.54)
Planck_lowl_TT	22.16	22.89 (−0.73)	23.25 (−1.09)
Pantheon	1027.28	1031.64 (−4.36)	1027.31 (−0.03)
bao_boss_dr12	4.79	5.38 (−0.59)	9.27 (−4.48)
bao_smallz_2014	3.14	5.31 (−2.17)	4.58 (−1.44)
absolute_M	11.47	6.57 (4.9)	6.85 (4.62)
H_0 (SH0ES)	8.54	3.31 (5.23)	4.34 (4.2)
H_0 (H0LiCOW)	4.69	1.88 (2.81)	2.43 (2.26)
H_0 (MEGAMASER)	2.25	1.04 (1.21)	1.29 (0.96)
Total	3835.71	3823.50 (12.21)	3822.19 (12.51)

Table I: Comparison of effective χ^2 between VCDM and ΛCDM for individual data sets.

	VCDM low$-z$	**VCDM high$-z$**	**ΛCDM**
Parameters	95% **limits**	95% **limits**	95% **limits**
β_H	$0.947^{+0.031}_{-0.037}$	≤ 0.80	−
A_2	$0.295^{+0.086}_{-0.052}$	$1.82^{+0.69}_{-0.93}$	−
$10^2\omega_{\rm b}$	$2.254^{+0.022}_{-0.032}$	$2.240^{+0.034}_{-0.024}$	$2.270^{+0.023}_{-0.029}$
$\tau_{\rm reio}$	$0.054^{+0.018}_{-0.013}$	$0.053^{+0.017}_{-0.014}$	$0.061^{+0.015}_{-0.017}$
n_s	$0.9677^{+0.0771}_{-0.0769}$	$0.9664^{+0.008}_{-0.009}$	$0.9736^{+0.0066}_{-0.0076}$
$10^{10}A_s$	$3.043^{+0.036}_{-0.028}$	$3.044^{+0.032}_{-0.032}$	$3.052^{+0.031}_{-0.036}$
H_0	$70.83^{+1.07}_{-1.13}$	$70.49^{+1.11}_{-1.09}$	$69.40^{+0.76}_{-0.8}$
$\Omega_{\rm m}$	$0.282^{+0.011}_{-0.009}$	$0.2865^{+0.0096}_{-0.0097}$	$0.2899^{+0.0101}_{-0.0092}$
M	$-19.34^{+0.03}_{-0.03}$	$-19.34^{+0.03}_{-0.03}$	$-19.37^{+0.02}_{-0.02}$

Table II: One-dimensional 2σ constraints for the cosmological parameters of interest after the estimation with the cosmological data sets considered.

$z \simeq 1.8$ respectively. As explained earlier, an intuitive picture from equation (6) gives the parameter β_H as the amplitude of the transition, A_2 the location of the redshift z at which the transition happens and A_3 is the width of such transition. It is clear from the choice of $H(z)$ that this is a low-redshift resolution for Hubble tension. Similar proposals have been made in [27–31]. Refer to [32] for a review of possible solutions to Hubble tension.

In this report we showed that the notorious H_0 tension can be addressed by a very minimal modification to the standard cosmological model, dubbed VCDM. We see that the value of $H_0^{\rm loc}$ estimated with this theory reduces the H_0 tension. It is also noticed that this model fits the cosmological data sets better than ΛCDM. On using Planck-Pantheon-BAO data alone we have seen two minima existing (which mostly differ by the value of redshift at which the transition in $H(z)$ occurs). On adding the three most recent measurements of H_0 (SH0ES, H0LiCOW and MEGAMASER) to the above chosen data sets, the two minima still exist with very similar values of χ^2 for each of them. These two minima not only differ, as already stated, by the value of the redshift where the $H(z)$ transition occurs, but also by the value of β_H (corresponding to the amplitude of the transition), but in any case $\beta_H < 1$ at 95% confidence level ($\beta_H = 1$ would make VCDM exactly coincide with ΛCDM). We find indeed that, compared to ΛCDM, the total fitness parameter is improved by $\Delta\chi^2 \simeq 12$. Background and perturbation variables are stable and finite. Hence we propose the VCDM model as a possible solution to the H_0 tension (giving the huge freedom for the choice of any wanted $H(z) > 0$, still compatible with a background evolution with no-ghosts, gradient instabilities, or extra fifth-force gravitational degrees of freedom). We need further investigation to look at whether VCDM can address the tension in the large-scale structure, S_8 along with the H_0 tension, although as already shown in [8], for this theory $G_{\rm eff}/G_N = 1$, at short scales. The behaviour of reducing H_0 tension within this theory sounds promising and it would be interesting to test this behaviour with future cosmology surveys like EUCLID [33] and LSST [34]. Finally we want to stress here that violations of 4D diffeo are only present in the gravity sector at cosmological scales. Since gravity is modified in the IR limit, and because of the absence of any extra gravita-

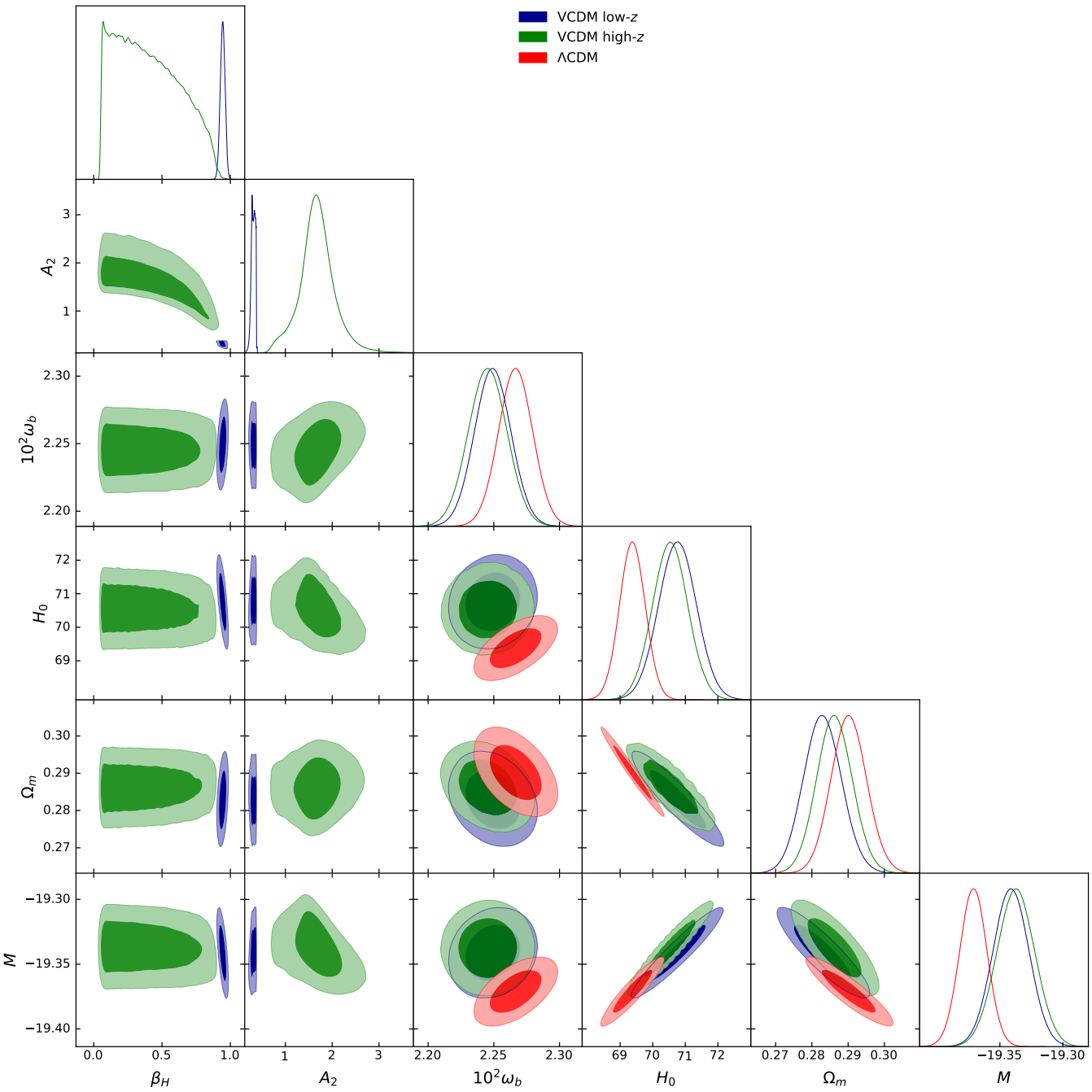


Figure 1: 2-dimensional marginalised likelihoods for the VCDM low$-z$, VCDM high$-z$ and ΛCDM model fitting against the cosmological data sets.

tional mode other than the standard tensorial gravitons, we expect that graviton loop corrections to be negligible. Therefore matter sector Lagrangians are fully covariant in 4D, up to $M_{\rm P}^2$-suppressed, tiny radiative corrections.

Appendix A: Calculation of $H_0^{\rm loc}$

Here we explain how to determine the local value of Hubble expansion rate today for a given theoretical model. We follow the method explained in [16, 17].

The apparent magnitude of a supernovae at a redshift

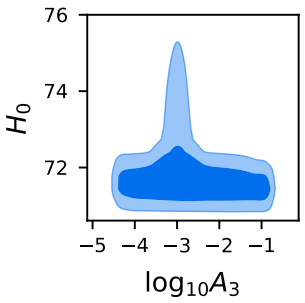


Figure 2: Degeneracy over the parameter A_3.

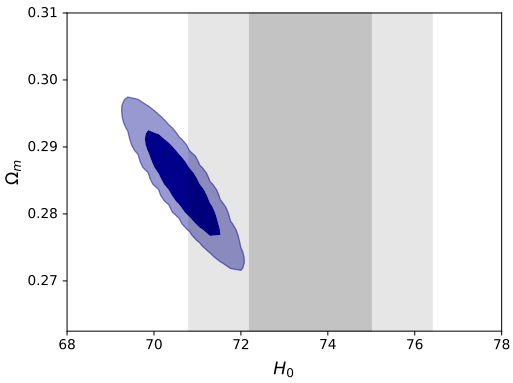


Figure 3: $\Omega_{\rm m} - H_0$ contour showing the H_0-tension is reduced compared with the local determination of $H_0^{\rm loc}$ within the VCDM theory. The black shade is $H_0^{\rm loc}$.

z is given by

$$m_B^t(z) = 5\log_{10}\left[\frac{d_L(z)}{1\text{Mpc}}\right] + 25 + M_B\,, \tag{A1}$$

where $d_L(z)$ is the luminosity distance and M_B is the absolute magnitude. The superscript t in $m_B^t(z)$ stands for theoretical apparent magnitude. The luminosity distance is given by

$$d_L = \frac{c}{H_0}(1+z)\int_0^z \frac{dz'}{E(z')}\,, \tag{A2}$$

where $E = H/H_0$. Then the apparent magnitude can be rewritten as

$$\begin{aligned} m_B^t &= 5\log_{10}\left[(1+z)\int_0^z \frac{dz'}{E(z')}\right] \\ &\quad -5\log_{10}\left[\frac{(1\text{Mpc})H_0}{c}\right] + 25 + M_B\,. \end{aligned} \tag{A3}$$

Now we define

$$\begin{aligned} \tilde{m}_B^t &= m_B^t - M_B + 5\log_{10}\left[\frac{(1\text{Mpc})H_0}{c}\right] \\ &= 5\log_{10}\left[(1+z)\int_0^z \frac{dz'}{E(z')}\right] + 25\,, \end{aligned} \tag{A4}$$

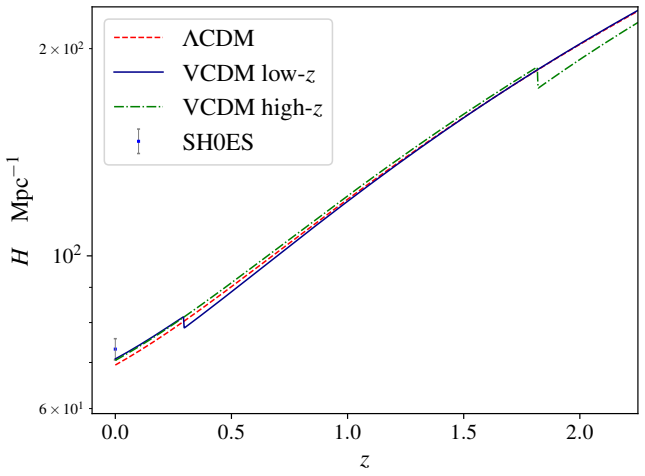


Figure 4: Zoomed version of H vs z plot. Here we can see two independent transitions in the $H(z)$ at very low redshift around $z \simeq 0.3$ and $z \simeq 1.8$.

which does not depend on both H_0 and M_B, but only on the dynamics of $E(z)$, which is a function of the other parameters of VCDM. We would then introduce the residual

$$m_{B,i} - m_{B,i}^t = m_{B,i} - \tilde{m}_{B,i}^t - M_B + 5\log_{10}\left[\frac{(1\text{Mpc})H_0}{c}\right],$$

to find a χ^2 distribution out of it. On calling

$$\begin{aligned} W_i &= m_{B,i} - \tilde{m}_{B,i}^t \\ &= m_{B,i} - \left(5\log_{10}\left[(1+z)\int_0^z \frac{dz'}{E(z')}\right] + 25\right), \end{aligned} \tag{A5}$$

we then need to find the residues on the variable

$$\begin{aligned} \chi^2 &= (m_{B,i} - m_{B,i}^t)\Sigma_{ij}^{-1}(m_{B,j} - m_{B,j}^t) \\ &= \left(W_i - M_B + 5\log_{10}\left[\frac{(1\text{Mpc})H_0}{c}\right]\right)\Sigma_{ij}^{-1} \\ &\quad \left(W_j - M_B + 5\log_{10}\left[\frac{(1\text{Mpc})H_0}{c}\right]\right). \end{aligned} \tag{A6}$$

Now consider

$$\bar{d}_L \equiv (1+z)\int_0^z \frac{dz'}{E(z')}\,, \tag{A7}$$

so that

$$\bar{d}_L' = \frac{dz}{dN}\frac{\bar{d}_L}{dz} = \bar{d}_L + \frac{(1+z)^2}{E(z)}\,, \tag{A8}$$

where we have used

$$\frac{dz}{dN} = 1 + z\,, \tag{A9}$$

considering $N = \ln(a_0/a) = \ln(1+z)$. Now we can solve for $\bar{d}_L(z)$, given the initial conditions $\bar{d}_L(0) = 0 = z(0)$.

Once we have the quantities $\bar{d}_L$ for any data-redshift, we have W_i so that we are able to find

$$S_0 \equiv V^T \Sigma^{-1} V \,, \tag{A10}$$

$$S_1 \equiv W^T \Sigma^{-1} V \,, \tag{A11}$$

where $V_i = 1$ and Σ_{ij} is the covariance matrix.

Finally, the mean value and the variance of $H_0^{\rm loc}$ can be determined by the log-normal distribution

$$H_0^{\rm loc} = e^{\mu_{\rm ln} + \frac{1}{2}\sigma^2_{\rm ln}} \,, \tag{A12}$$

$$\sigma^2_{H_0^{\rm loc}} = \left(e^{\sigma^2_{\rm ln}} - 1\right) e^{2\mu_{\rm ln} + \sigma^2_{\rm ln}} \,, \tag{A13}$$

where

$$\mu_{\rm ln} = \frac{\ln 10}{5}\left[\bar{M}_B + \frac{\ln 10}{5}\left(\sigma_M^2 + \frac{1}{S_0}\right) - \frac{S_1}{S_0}\right] , \tag{A14}$$

$$\sigma_{\rm ln} = \frac{\ln 10}{5}\sqrt{\sigma_M^2 + \frac{1}{S_0}} \,, \tag{A15}$$

which, in turn, only depends on M_B, σ_M^2, S_0 and S_1. Also one should notice that S_0 is only given by the data, and it does not depend on the model, but S_1 does depend on the values of $\bar{d}_L$'s, and this will affect $H_0^{\rm loc}$ for different models. To get a log-normal distribution we assumed a Gaussian distribution for M_B and have marginalized over it (refer to [16] for details).

Now we select the the supernovae data and the covariance matrix from Pantheon[4] dataset up to $z \leq 0.15$, according to [16]. Then we integrate the luminosity distance with respect to N to find S_1. From [16] we use the values $\bar{M}_B = -19.2322$ and $\sigma_M = 0.0404$. Hence we find the values of $H_0^{\rm loc}$ and $\sigma^2_{H_0^{\rm loc}}$.

Further study is necessary to understand whether this late time change can fully address today's cosmological puzzles, including the S_8 tension. However, we think this study might help people focusing their efforts on finding the best profile for $H(z)$ which can model the data sets.

We thank George Efstathiou for useful comments. The work of A.D.F. was supported by Japan Society for the Promotion of Science Grants-in-Aid for Scientific Research No. 20K03969. The work of S.M. was supported by JSPS KAKENHI Grant Numbers 17H02890, 17H06359, and by WPI MEXT, Japan. M.C.P. acknowledges the support from the Japanese Government (MEXT) scholarship for Research Student. Numerical computation in this work was carried out at the Yukawa Institute Computer Facility.

* antonio.defelice@yukawa.kyoto-u.ac.jp

† shinji.mukohyama@yukawa.kyoto-u.ac.jp

‡ masroor.cp@yukawa.kyoto-u.ac.jp

[4] https://github.com/dscolnic/Pantheon

[1] Adam G. Riess, Stefano Casertano, Wenlong Yuan, Lucas M. Macri, and Dan Scolnic. Large Magellanic Cloud Cepheid Standards Provide a 1% Foundation for the Determination of the Hubble Constant and Stronger Evidence for Physics beyond ΛCDM. *Astrophys. J.*, 876(1):85, 2019.

[2] Kenneth C. Wong et al. H0LiCOW XIII. A 2.4% measurement of H_0 from lensed quasars: 5.3σ tension between early and late-Universe probes. 7 2019.

[3] M.J. Reid, J.A. Braatz, J.J. Condon, L.J. Greenhill, C. Henkel, and K.Y. Lo. The Megamaser Cosmology Project: I. VLBI observations of UGC 3789. *Astrophys. J.*, 695:287–291, 2009.

[4] Wendy L. Freedman et al. The Carnegie-Chicago Hubble Program. VIII. An Independent Determination of the Hubble Constant Based on the Tip of the Red Giant Branch. 7 2019.

[5] N. Aghanim et al. Planck 2018 results. VI. Cosmological parameters. 7 2018.

[6] Jose Luis Bernal, Licia Verde, and Adam G. Riess. The trouble with H_0. *JCAP*, 10:019, 2016.

[7] Adam G. Riess. The Expansion of the Universe is Faster than Expected. *Nature Rev. Phys.*, 2(1):10–12, 2019.

[8] Antonio De Felice, Andreas Doll, and Shinji Mukohyama. A theory of type-II minimally modified gravity. *JCAP*, 09:034, 4 2020.

[9] Andrew R Liddle. Information criteria for astrophysical model selection. *Mon. Not. Roy. Astron. Soc.*, 377:L74–L78, 2007.

[10] N. Aghanim et al. Planck 2018 results. V. CMB power spectra and likelihoods. 2019.

[11] Florian Beutler, Chris Blake, Matthew Colless, D. Heath Jones, Lister Staveley-Smith, Lachlan Campbell, Quentin Parker, Will Saunders, and Fred Watson. The 6dF Galaxy Survey: Baryon Acoustic Oscillations and the Local Hubble Constant. *Mon. Not. Roy. Astron. Soc.*, 416:3017–3032, 2011.

[12] Ashley J. Ross, Lado Samushia, Cullan Howlett, Will J. Percival, Angela Burden, and Marc Manera. The clustering of the SDSS DR7 main Galaxy sample – I. A 4 per cent distance measure at $z = 0.15$. *Mon. Not. Roy. Astron. Soc.*, 449(1):835–847, 2015.

[13] Shadab Alam et al. The clustering of galaxies in the completed SDSS-III Baryon Oscillation Spectroscopic Survey: cosmological analysis of the DR12 galaxy sample. *Mon. Not. Roy. Astron. Soc.*, 470(3):2617–2652, 2017.

[14] D.M. Scolnic et al. The Complete Light-curve Sample of Spectroscopically Confirmed SNe Ia from Pan-STARRS1 and Cosmological Constraints from the Combined Pantheon Sample. *Astrophys. J.*, 859(2):101, 2018.

[15] Adam G. Riess, Stefano Casertano, Wenlong Yuan, J. Bradley Bowers, Lucas Macri, Joel C. Zinn, and Dan Scolnic. Cosmic Distances Calibrated to 1% Precision with Gaia EDR3 Parallaxes and Hubble Space Telescope Photometry of 75 Milky Way Cepheids Confirm Tension with ΛCDM. *Astrophys. J. Lett.*, 908(1):L6, 2021.

[16] David Camarena and Valerio Marra. Local determination of the Hubble constant and the deceleration parameter. *Phys. Rev. Res.*, 2(1):013028, 2020.

[17] Giampaolo Benevento, Wayne Hu, and Marco Raveri. Can Late Dark Energy Transitions Raise the Hubble constant? *Phys. Rev. D*, 101(10):103517, 2020.

[18] David Camarena and Valerio Marra. On the use of the local prior on the absolute magnitude of Type Ia supernovae in cosmological inference. 1 2021.

[19] George Efstathiou. To H0 or not to H0? 3 2021.

[20] N. Aghanim et al. Planck intermediate results. LI. Features in the cosmic microwave background temperature power spectrum and shifts in cosmological parameters. *Astron. Astrophys.*, 607:A95, 2017.

[21] Pavel Motloch and Wayne Hu. Lensinglike tensions in the *Planck* legacy release. *Phys. Rev. D*, 101(8):083515, 2020.

[22] Diego Blas, Julien Lesgourgues, and Thomas Tram. The Cosmic Linear Anisotropy Solving System (CLASS) II: Approximation schemes. *JCAP*, 1107:034, 2011.

[23] Masroor C. Pookkillath, Antonio De Felice, and Shinji Mukohyama. Baryon Physics and Tight Coupling Approximation in Boltzmann Codes. *Universe*, 6:6, 2020.

[24] Benjamin Audren, Julien Lesgourgues, Karim Benabed, and Simon Prunet. Conservative Constraints on Early Cosmology: an illustration of the Monte Python cosmological parameter inference code. *JCAP*, 1302:001, 2013.

[25] Thejs Brinckmann and Julien Lesgourgues. MontePython 3: boosted MCMC sampler and other features. *Phys. Dark Univ.*, 24:100260, 2019.

[26] Antony Lewis. GetDist: a Python package for analysing Monte Carlo samples. 10 2019.

[27] Ryan E. Keeley, Shahab Joudaki, Manoj Kaplinghat, and David Kirkby. Implications of a transition in the dark energy equation of state for the H_0 and σ_8 tensions. *JCAP*, 12:035, 2019.

[28] Kyriakos Vattis, Savvas M. Koushiappas, and Abraham Loeb. Dark matter decaying in the late Universe can relieve the H0 tension. *Phys. Rev. D*, 99(12):121302, 2019.

[29] Gongjun Choi, Motoo Suzuki, and Tsutomu T. Yanagida. Quintessence Axion Dark Energy and a Solution to the Hubble Tension. *Phys. Lett. B*, 805:135408, 2020.

[30] Antonio De Felice, Chao-Qiang Geng, Masroor C. Pookkillath, and Lu Yin. Reducing the H_0 tension with generalized Proca theory. *JCAP*, 08:038, 2020.

[31] Andrzej Hryczuk and Krzysztof Jodłowski. Self-interacting dark matter from late decays and the H_0 tension. *Phys. Rev. D*, 102(4):043024, 2020.

[32] Eleonora Di Valentino, Olga Mena, Supriya Pan, Luca Visinelli, Weiqiang Yang, Alessandro Melchiorri, David F. Mota, Adam G. Riess, and Joseph Silk. In the Realm of the Hubble tension − a Review of Solutions. 3 2021.

[33] Luca Amendola et al. Cosmology and fundamental physics with the Euclid satellite. *Living Rev. Rel.*, 16:6, 2013.

[34] Alexandra Abate et al. Large Synoptic Survey Telescope: Dark Energy Science Collaboration. 11 2012.